

This article was downloaded by:

On: 25 January 2011

Access details: *Access Details: Free Access*

Publisher *Taylor & Francis*

Informa Ltd Registered in England and Wales Registered Number: 1072954 Registered office: Mortimer House, 37-41 Mortimer Street, London W1T 3JH, UK



Liquid Crystals

Publication details, including instructions for authors and subscription information:

<http://www.informaworld.com/smpp/title~content=t713926090>

Concentration dependences of dielectric properties at 10^5 Hz and 10^6 Hz for aqueous solutions of hydroxypropyl cellulose

Katsufumi Tanaka^a; Takatoshi Morina^b; Yuichiro Tanabe^a; Ryuichi Akiyama^a

^a Department of Macromolecular Science and Engineering, Graduate School of Science and Technology, Kyoto Institute of Technology, Matsugasaki, Kyoto 606-8585, Japan ^b Department of Polymer Science and Engineering, Kyoto Institute of Technology, Matsugasaki, Kyoto 606-8585, Japan

To cite this Article Tanaka, Katsufumi , Morina, Takatoshi , Tanabe, Yuichiro and Akiyama, Ryuichi(2007) 'Concentration dependences of dielectric properties at 10^5 Hz and 10^6 Hz for aqueous solutions of hydroxypropyl cellulose', *Liquid Crystals*, 34: 9, 1019 – 1028

To link to this Article: DOI: 10.1080/02678290701603031

URL: <http://dx.doi.org/10.1080/02678290701603031>

PLEASE SCROLL DOWN FOR ARTICLE

Full terms and conditions of use: <http://www.informaworld.com/terms-and-conditions-of-access.pdf>

This article may be used for research, teaching and private study purposes. Any substantial or systematic reproduction, re-distribution, re-selling, loan or sub-licensing, systematic supply or distribution in any form to anyone is expressly forbidden.

The publisher does not give any warranty express or implied or make any representation that the contents will be complete or accurate or up to date. The accuracy of any instructions, formulae and drug doses should be independently verified with primary sources. The publisher shall not be liable for any loss, actions, claims, proceedings, demand or costs or damages whatsoever or howsoever caused arising directly or indirectly in connection with or arising out of the use of this material.

Concentration dependences of dielectric properties at 10^5 Hz and 10^6 Hz for aqueous solutions of hydroxypropyl cellulose

KATSUFUMI TANAKA*†, TAKATOSHI MORINA‡, YUICHIRO TANABE† and RYUICHI AKIYAMA†

†Department of Macromolecular Science and Engineering, Graduate School of Science and Technology, Kyoto Institute of Technology, Matsugasaki, Kyoto 606-8585, Japan

‡Department of Polymer Science and Engineering, Kyoto Institute of Technology, Matsugasaki, Kyoto 606-8585, Japan

(Received 24 April 2007; accepted 25 June 2007)

The concentration dependences of dielectric properties measured at 10^5 Hz and 10^6 Hz are reported for aqueous solutions of hydroxypropyl cellulose. Phase behaviour of the solutions was also observed with a polarizing optical microscope. For solutions with concentrations well above 40 wt %, polydomain textures, including the banded texture, were observed after a prehistory of deformation. No significant discontinuous changes in the dielectric constant, ϵ_r' , and loss factor, ϵ_r'' , were found at the concentrations around the onset of the isotropic–cholesteric phase transition and in the biphasic region. In contrast, the steeper changes in ϵ_r' and ϵ_r'' were found at the critical concentration for the fully developed cholesteric phase transition with the polydomain textures.

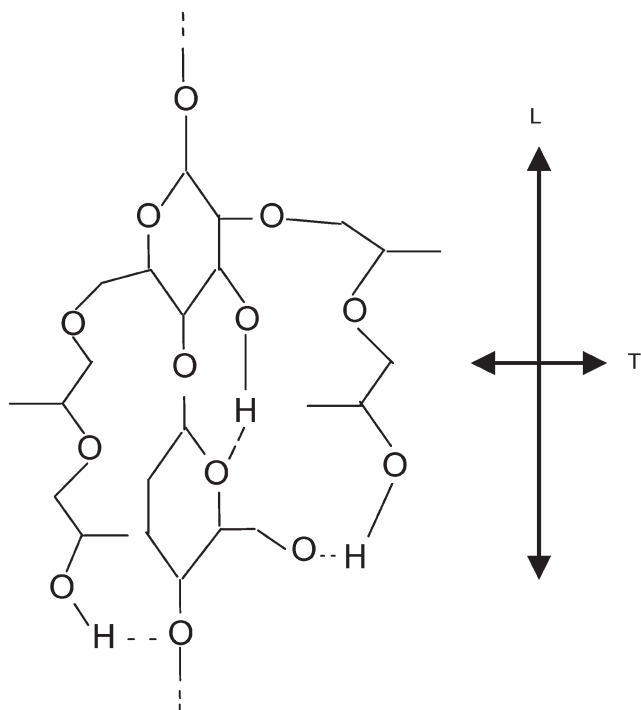
1. Introduction

Hydroxypropyl cellulose (HPC) is known as a lyotropic liquid crystal with cholesteric phase structure in concentrated solutions [1, 2]. The polymer is soluble in cold water as well as organic solvents. The anisotropic mesophase of the polymer shows significant optical properties, such as iridescence, birefringence, optical rotational dispersion, and so on [1–3]. The phase behaviour of aqueous solutions of HPC is dependent on both temperature and concentration [2]. The critical concentration for the isotropic–cholesteric phase transition was reported to be about 40 wt % at room temperature, whereas a phase separation was observed at about 40°C. Later studies showed that the critical concentration around 40 wt % showed the onset of mesophase formation, and that the coexistence of an isotropic and an ordered phase was still possible at higher concentrations. The upper concentration limit of the biphasic region was reported to be 47 wt % at 20°C [4] and at room temperature [5]. The updated phase diagram related to both temperature and concentration was also reported with high resolution using video-enhanced contrast optical microscopy, showing a narrow biphasic gap below about 18°C. In the phase diagram, the upper concentration limit of the biphasic region can also be obtained around 47 wt % at 17°C [6].

Significantly, iridescence was found for solutions with concentrations from around 50 wt % to 70 wt %, and the colour correspondingly moved to the violet end of the spectrum with increasing concentration. The solution became gel-like (or highly viscous fluids of the cholesteric phase [4]) at concentrations higher than 70 wt %, and it became clear film as the concentration further increased [2].

It is worthwhile to note that the HPC molecules act like rigid rods in certain solutions, although the molecule consists of a linear chain of β -(1,4)-linked anhydroglucose units with non-mesogenic substituents on the hydroxyl groups. This fact is generally explained by the intramolecular hydrogen bonding in HPC in solutions. An extensive study, including the superstructure of HPC with intramolecular hydrogen bonding, was reported for the solid film cast from aqueous solutions [7]. In figure 1, a schematic representation is shown for a portion of an HPC molecule showing intramolecular hydrogen bonding. On average, each monomer unit in the HPC backbone is substituted with four poly(propylene oxide) mer units (MS=4). The idealized molecular model of the HPC molecule was constructed under the assumption that the backbone of the molecule was a helix composed of three anhydroglucose units (rings) per repeat, and that each monomer unit contained two branches, two propylene oxide units in length. The high degree of intramolecular hydrogen bonding is widely assumed to explain why the HPC

*Corresponding author. Email: ktanaka@kit.ac.jp



Moles of substitution: 4

Figure 1. Schematic representation of a portion of an HPC molecule showing intramolecular hydrogen bonding.

molecule exists as a nearly linear rod in solution. However, the HPC molecule in water was reported to behave as intermediate between rod-like molecules and random coils [8]. In solution, the phase separation and coexistence of isotropic and anisotropic phases for relatively flexible HPC molecules are predicted by a model in which rigid rods are replaced by freely joined rods, the length of which equals the Kuhn equivalent segment length of the polymer chain [2].

Dielectric properties of HPC have been reported mostly for solid films produced by a hydraulic press [9–11]. The dielectric relaxation phenomena of moistened and dry polysaccharides were studied, and the dielectric constant of the moistened solid film of HPC was reported to be larger than that of the dried film at room temperature. Further, the dielectric loss related to a secondary relaxation was sensitively affected by the presence of even a small amount of water [9]. The observed secondary relaxations were extensively studied in relation to a local motion of chain segments via the glycosidic linkages [10]. The dielectric properties have also been reported for the solid film cast from aqueous solutions of HPC [12].

On the other hand, studies on the dielectric properties of HPC in solutions are limited [13]. The dielectric

behaviour of HPC in dioxane was studied for isotropic as well as anisotropic solutions. The dielectric parameters of the relaxation, which were found at frequencies on the order from 10 Hz to 10^3 Hz and at several temperatures, changed discontinuously around a critical concentration corresponding to the isotropic–cholesteric phase transition. The relaxation was discussed and related to limited angular diffusion of rods within a virtual cone prescribed by the neighbouring molecules in the anisotropic phase [13–16]. In the isotropic state, rotational diffusion of a rigid rod of the longitudinal axis, as shown in figure 1, is possible with a 4π solid angle, whereas diffusion in the lyotropic nematic state is partially limited within a virtual cone to reduce the relaxation magnitude. For aqueous solutions of HPC, there seems to be no systematic study on the dielectric properties. Especially, the concentration dependences of the dielectric constant and loss factor are not available in the literature so far. Dielectric relaxation at lower frequencies of a highly polar system is usually affected by electrode polarization and ionic conduction [14, 17], and important relaxations are often screened out at lower frequencies. On the other hand, the electrode polarization and ionic conduction would be reduced at higher frequencies of 10^5 Hz and 10^6 Hz. Further, the rotational diffusion of a partially flexible rod with side chains of the transversal axis, as shown in figure 1, would respond at the higher frequencies. The local motion of chain segments in the relatively flexible rod would also be detectable as the longitudinal component and/or transversal component, even confined in the concentrated solutions.

In addition, it is generally known that monodomain texture with homeotropic or homogeneous molecular alignments cannot easily be prepared for liquid crystalline polymers including HPC. Instead, the anisotropic solutions of liquid crystalline polymers essentially show polydomain textures in the quiescent state [5], and shear-induced textures or banded texture after shearing [18, 19]. These macroscopic textures are closely related to the macroscopic physical properties, such as flow behaviour in the presence [20] or absence [18] of an electric field. Therefore, the macroscopic textures would also be related to the dielectric properties, although the textures have not been taken into account so far for the dielectric properties of HPC solutions.

It is of great interest for us to study the concentration dependences of the dielectric properties for aqueous solutions of HPC partly because the dependences are expected to provide insight into the molecular motions in the isotropic and cholesteric phases, as well as the lyotropic transition. In view of materials engineering, the dependences would be related to the preparation

process of solid films cast from aqueous solutions. The dependences are also expected to provide an in-situ monitoring method for the process. In the present paper, the concentration dependences of the dielectric constant and loss factor are reported for aqueous solutions of HPC measured at frequencies of 10^5 Hz and 10^6 Hz. In a subsequent paper [21], in-situ monitoring with the dielectric properties will be reported for the preparation process of solid films cast from aqueous solutions of HPC.

2. Experimental

Hydroxypropyl cellulose was purchased from Sigma-Aldrich, Inc. The weight-averaged molecular weight, M_w , was approximately 80 000, and the number-averaged molecular weight, M_n , was approximately 10 000. From the supplier data, MS (moles of substitution) was 3.5, which is defined as average number of moles of propylene oxide attached to a monomer unit. Further, the viscosity of the aqueous solution at polymer concentration of 10 wt% at 25°C was 0.463 Pa s, and the pH of the aqueous solution of 2 wt% was 5.47. Distilled water was used to prepare solutions with polymer concentrations from 10 to 80 wt%. The sample solutions were kept for at least three weeks in a desiccator at room temperature (around 17°C). Solid films with film thickness around 0.6 mm were also cast from aqueous solutions of HPC at room temperature.

Anisotropic texture was observed at room temperature using a polarizing optical microscope (Nikon, Optiphot2-Pol) equipped with a digital camera. Usually, a small amount of solution was placed and slightly compressed and/or sheared between a slide glass and a cover glass without spacer. For further observations of the biphasic texture, a cover glass was carefully mounted on the solution of 45 wt%. In addition, the solution of 80 wt% was sheared a little more intensely using another slide glass for shear-induced textures.

The dielectric properties of sample solutions were measured using an impedance analyser (HP, 4192A) with a cell for liquid samples (Yokogawa, LE-21), as shown in figure 2. The cell was composed of the low-potential electrode (L) and high-potential electrode (H), and the assembly was electrically insulated from the outer jacket, which was connected to ground via guard electrode. In the dielectric measurements, the lower part of the cell with high-potential electrode (H) was filled with a sample solution of approximately 1 ml. The upper lid with the low-potential electrode (L) and guard electrode was inserted and attached to the lower part of the cell by a screw. To some extent, the sample solution was deformed by compression and/or shear. In our cell,

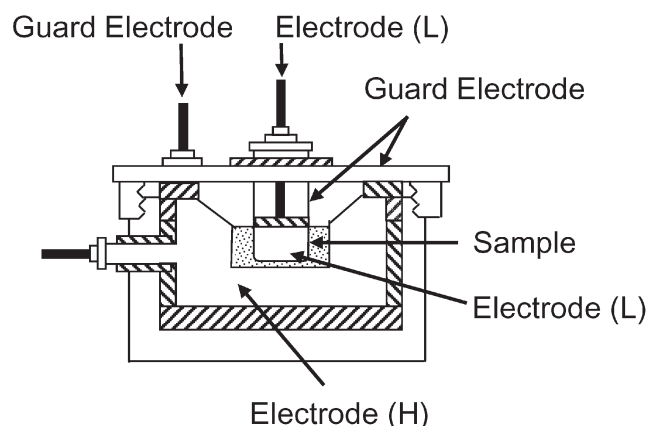


Figure 2. The dielectric cell for solutions.

the upper lid is not completely sealed, and slight evaporation of the solvent cannot be avoided. Therefore, the sample solutions were not matured much longer than 30 min in the cell. Instead, a set of the dielectric measurements was performed for each sample solution immediately and approximately 30 min after the cell was filled with the solution at room temperature, which showed no significant evaporation of the solvent in the present study.

The dielectric constant, ϵ_r' , and loss factor, ϵ_r'' , of a sample solution were calculated from the following equations:

$$\epsilon_r' = (C_s - C_f) / (C_a - C_f), \quad (1)$$

$$\epsilon_r'' = G_s / [2\pi\nu(C_a - C_f)], \quad (2)$$

where C_s and G_s are, respectively, the capacitance and conductance of the sample, C_a is the capacitance of the empty cell and ν is the frequency. Before each measurement, C_f was determined for calibration using equation (1) with a reference sample of well-defined temperature dependence of ϵ_r' . In the present study, sufficiently dried hexane [22] was used for the calibration.

The solid films were also measured in our laboratory using the impedance analyser equipped with a dielectric test fixture (HP, 16451B) with an electrode diameter of 38 mm. The solid films were independently measured using an impedance analyser (TA Instruments, DEA2970) equipped with a similar dielectric test fixture with an electrode diameter of 25 mm. The latter measurements were performed at a laboratory of TOSOH Analysis and Research Centre Co. The dielectric constant and loss factor of a solid film were simply calculated using the capacitance and conductance of the sample with the thickness and electrode diameter.

3. Results and discussion

3.1. Optical observations

The phase behaviour of the solutions was observed with a polarizing optical microscope. As discussed in section 2, the sample solution in the dielectric cell was essentially deformed to some extent by compression and/or shear. Therefore, it would be helpful to observe the solutions with deformation prehistory. Polarized optical micrographs obtained during usual observation are shown in figure 3. For the solution of 40 wt% HPC, an optically anisotropic portion was found, as shown in figure 3 a, although the anisotropic texture was rather unstable and affected by the deformation prehistory. The concentration is consistent with the onset of the isotropic–cholesteric phase transition observed using the polarizing optical microscopy [2, 4, 5]. For the solutions with concentrations well above 40 wt%, apparently stable anisotropic textures were observed. As shown in figures 3 b–3 d, the observed anisotropic textures are not monodomain but polydomain in nature. It should be pointed out that the solution of 45 wt% was reported to be biphasic and that of 50 wt% to be fully anisotropic with cholesteric structure at room temperature [4–6].

In figure 3 b, no biphasic characteristics can be seen for the solution of 45 wt%, and the polydomain textures shown in figures 3 b–3 d look like the banded texture [18]. Therefore, further optical observations were performed. For observations of the biphasic characteristics, a cover glass was carefully mounted on the solution of 45 wt%. In figure 4 a, small anisotropic spherulites were found in the solution of 45 wt% during

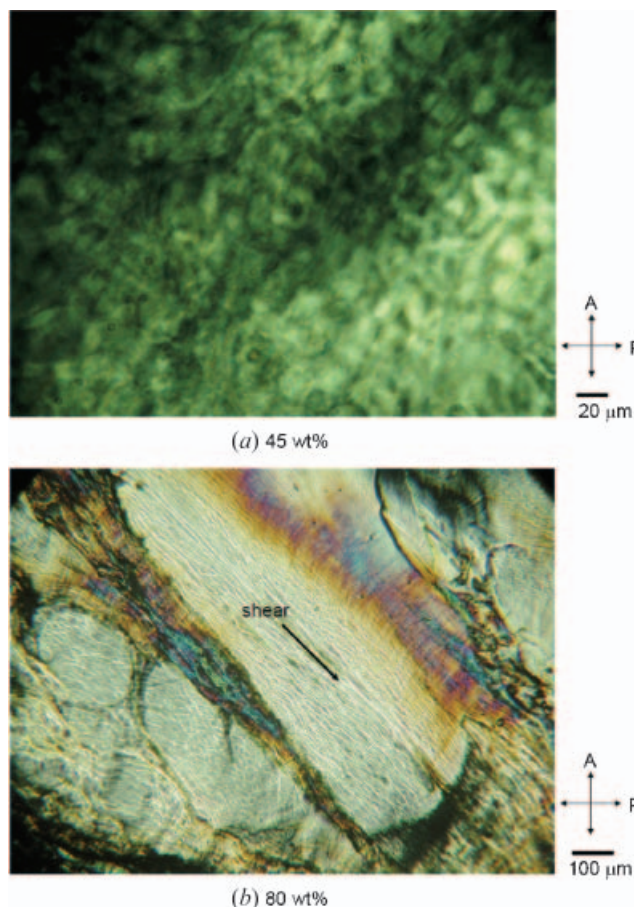


Figure 4. Polarized optical micrographs for the solutions with concentrations of 45 wt% (a) and 80 wt% (b) of HPC. For the solution of 45 wt%, a cover glass was carefully mounted on the solution. The solution of 80 wt% was sheared in the direction shown in the micrograph.

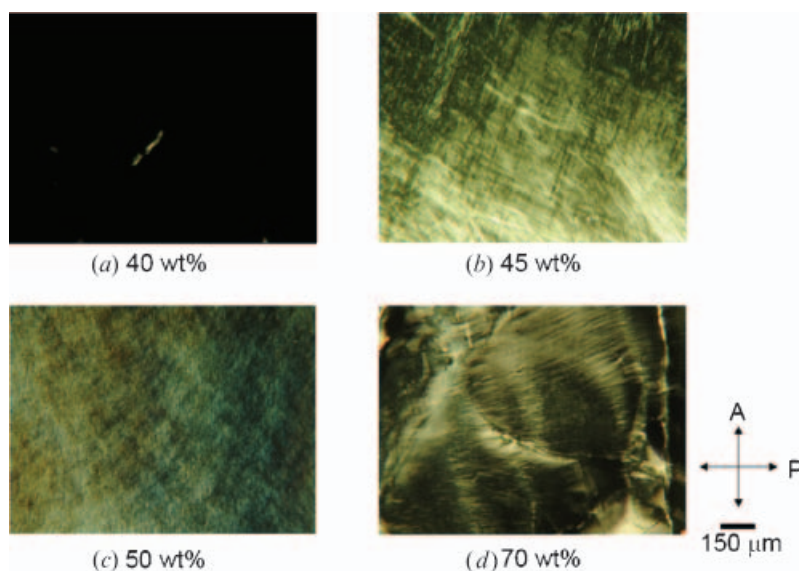


Figure 3. Polarized optical micrographs for the solutions with various concentrations of HPC with prehistory of deformation.

the observations. The observed anisotropic spherulites are similar to those observed by Fried and Sixou [5], suggesting the biphasic state. Further, the anisotropic spherulites were extremely sensitive to only a weak compression and/or shear deformation, and they were easily deformed into a thread-like texture. On the other hand, the solution of 80 wt% was sheared a little more intensely using another slide glass for shear-induced textures. In figure 4 b, two significant textures can be observed, the bright texture oriented along the shear and the banded texture developed perpendicular to the shear. It is worthwhile to note that the bright texture oriented along the shear was apparently stable during the optical observation for the concentrated and highly viscous solution of 80 wt% HPC. For anisotropic solutions with much lower concentrations and viscosities, the oriented portion was relatively unstable and the relaxation of the shear-induced orientation was observed easily.

In addition, the anisotropic solutions also showed the iridescence representing the cholesteric structure. The solution of 50 wt% HPC showed a red iridescence, and the colour correspondingly moved to the violet end of the spectrum with increasing concentration up to 70 wt%, which agrees fairly well with previous observations [2, 4].

3.2. Dielectric relaxation behaviour

The dielectric constant, ϵ_r' , is plotted logarithmically in figure 5 a against frequency for the solutions with various concentrations of HPC. (In figure 5, results below 90 Hz are not shown because the values were extremely large and some data were unstable. In the measurement of the solution of 80 wt%, tiny air bubbles were not removed completely when the cell was filled with the highly viscous solution.) For a solution with a given concentration, ϵ_r' at lower frequencies is still extremely large and it decreases steeply up to around 10^5 Hz and then decreases gradually. In figure 5 b, ϵ_r'' at lower frequencies is also extremely large and it decreases up to higher frequencies on the order of 10^6 Hz. These results suggest that the dielectric relaxation at lower frequencies is affected by the electrode polarization and ionic conduction [14, 17], and an important relaxation reported for the HPC in dioxane [13] would be screened out at lower frequencies. On the other hand, only a slight decrease in ϵ_r' for a solution is found at frequencies higher than 10^5 Hz. Therefore, the electrode polarization and ionic conduction would be small at the higher frequencies. The frequency dependence of ϵ_r'' suggests that the effect of the dc conduction, which is briefly discussed later, is significant at lower

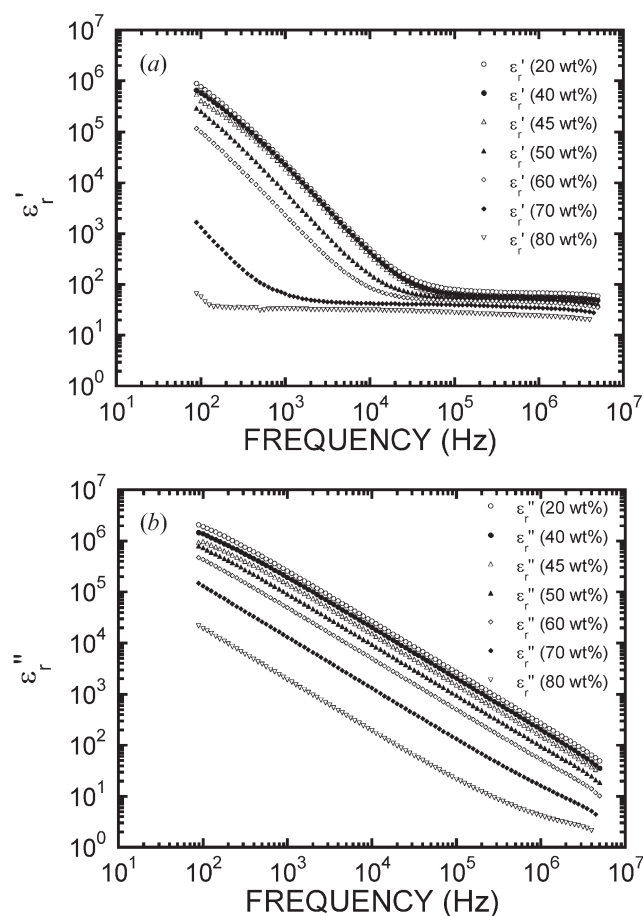


Figure 5. The dielectric constant (a) and loss factor (b) plotted logarithmically against frequency for the solutions with various concentrations of HPC.

frequencies, but the effect is relatively small at the higher frequencies of 10^5 Hz and 10^6 Hz.

At a given frequency from 10^3 Hz to 10^4 Hz, at which the data shown in figure 5 a (or 5 b) are easy to compare, the solutions with concentrations below 45 wt% show fairly close values of ϵ_r' (or ϵ_r''). On the other hand, the solution of 50 wt% HPC shows a steep decrease in ϵ_r' (or ϵ_r''), as shown in figure 5 a (or 5 b). Further, the relaxation frequency for concentrated solutions above 50 wt% is shifted to lower frequencies. These results suggest that the dielectric properties critically changed around the concentration of 50 wt%, slightly above the upper concentration limit for biphasic state.

In figure 5 b, the solution of 70 wt% shows a typical frequency dependence suggesting the effect of the dc conduction for ϵ_r'' , because ϵ_r'' at lower frequencies is mostly proportional to ν^{-1} . Further, ϵ_r' at lower frequencies, shown in figure 5 a, is mostly proportional to ν^{-2} , which would be related to the electrode polarization. Therefore, corrections for these effects

are needed using the following equations [14]:

$$\varepsilon_r''(\text{corrected}) = \varepsilon_r'' - \sigma_{\text{dc}}/2\pi\nu\varepsilon_0, \quad (3)$$

$$\varepsilon_r'(\text{corrected}) = \varepsilon_r' - \delta/\nu^2, \quad (4)$$

where σ_{dc} is the specific conductivity (S m^{-1}), ε_0 is the permittivity of free space and δ is an adjustable parameter. The lower-frequency data of ε_r'' and ε_r' were fitted with equations (3) and (4) to determine σ_{dc} and δ , respectively. Thus, corrected portions of $\varepsilon_r'(\text{corrected})$ and $\varepsilon_r''(\text{corrected})$ are plotted logarithmically against frequency in figures 6a and 6b, respectively. In figure 6, broad relaxations around 10^6 Hz and at frequencies lower than 10^4 Hz are suggested, although the data at lower frequencies may not be corrected sufficiently. However, the relaxation frequencies reported for the longitudinal rotational-diffusion for HPC in dioxane [13] are of the order from 10 Hz to 10^3 Hz, which qualitatively corresponds to the lower-frequency relaxation shown in

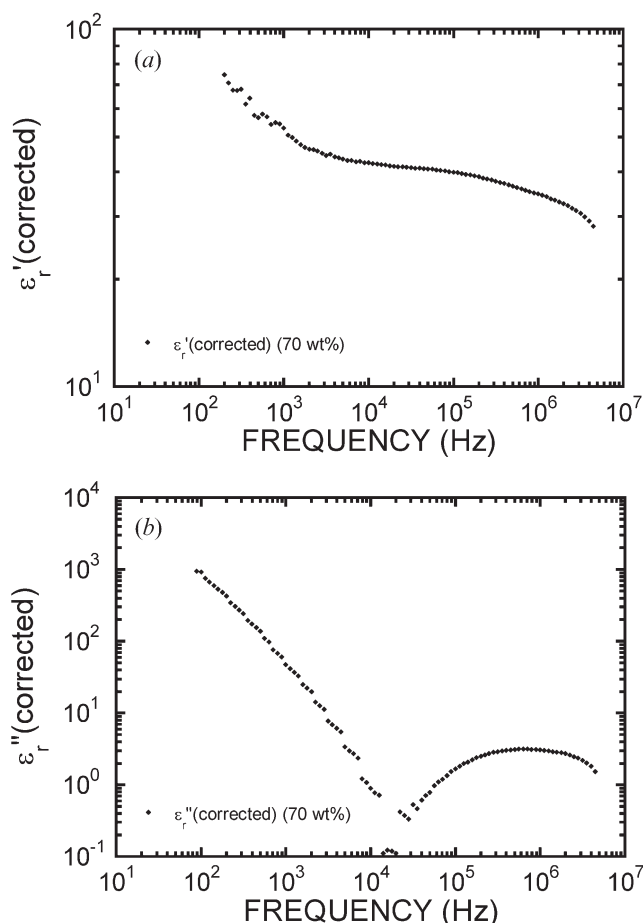


Figure 6. Corrected dielectric constant (a) and loss factor (b) plotted logarithmically against frequency for the solution of 70 wt% shown in figure 5.

figure 6. Further, it is expected that the broad relaxation around 10^6 Hz corresponds to the transversal rotational-diffusion for HPC in water.

Theoretically, the relaxation times of molecular rotation for a prolate spheroid with the major and minor axes of $2a$ and $2b$, respectively, can be obtained as follows [23]:

$$\frac{\tau_1}{\tau_0} = \frac{2}{3} \frac{1 - \rho^4}{(2 - \rho^2) \frac{\rho^2}{(1 - \rho^2)^{1/2}} \ln \frac{1 + (1 - \rho^2)^{1/2}}{\rho} - \rho^2}, \quad (5)$$

$$\frac{\tau_2}{\tau_0} = \frac{4}{3} \frac{1 - \rho^4}{(2\rho^2 - 1) \frac{\rho^2}{(1 - \rho^2)^{1/2}} \ln \frac{1 + (1 - \rho^2)^{1/2}}{\rho} + 1}, \quad (6)$$

$$\tau_0 = \frac{4\pi ab^2 \eta}{kT}, \quad (7)$$

where $\rho = b/a$, τ_1 and τ_2 are, respectively, the relaxation times of molecular rotation about the minor and major axes of the ellipsoid, τ_0 is the relaxation time for a sphere of the same volume, η ($=1 \times 10^{-3}$ Pa s) is the viscosity of the solvent, k is the Boltzmann constant, and T ($=290$ K) is the absolute temperature. The corresponding relaxation frequencies (ν_i ; $i=1, 2$) can also be defined as $\nu_i = (2\pi\tau_i)^{-1}$ [24].

In the calculation of ρ , the diameter of the molecule of 0.8 nm was assumed to $2b$, which was determined for water-cast films [7]. The length of the rod-like molecule was also assumed to $2a$, the value of which is 1 nm times the degree of polymerization (for $MS=4$), considering that there are three anhydroglucose units (rings) per 1.5 nm repeat [7]. For the sample of HPC provided, the molecular weight distribution would be broad because M_w/M_n is around 8. Therefore, the degree of polymerization was estimated from both M_w and M_n . The estimated lengths of the rod-like molecule were approximately 150 nm and 19 nm, respectively, from M_w and M_n . The relaxation frequencies ν_1 and ν_2 were then estimated to be 2×10^3 Hz and 3×10^6 Hz, respectively, from M_w . From M_n , ν_1 and ν_2 were also estimated to be 6×10^5 Hz and 2.5×10^7 Hz, respectively. In the estimation, the flexibility of the molecule was not taken into account.

Interestingly, ν_1 and ν_2 estimated from M_w are close to the broad relaxations shown in figure 6, whereas ν_1 and ν_2 estimated from M_n are acceptably overestimated. It should be noted that the assumption of an isolated rigid ellipsoid in water predicts the relaxation frequencies in diluted solutions, and that the overestimations for the relaxation frequencies are fairly acceptable in the case of the concentrated solution of 70 wt% dissolving partially flexible rod-like molecules. For concentrated

solutions, the angular diffusion of a rod is considered to be limited within a space of virtual cone [13–16]. It would be natural that the rotational diffusion of a rod is also restricted on a time scale to increase relaxation times (or to reduce relaxation frequencies) for the concentrated solutions. Similarly, the molecular motions related to the primary and secondary dispersions for the solid films would be significantly restricted. For instance, the reported relaxation frequency for the primary dispersion (α_a) was around 4×10^2 Hz or lower at 290 K [12]. Further, the relaxation frequency for an overlapped secondary dispersion of β and γ relaxations was around 5×10^5 Hz at 290 K [11], the responsible molecular origins of which were assigned to local chain relaxation and side-group relaxation, respectively [10]. Further, the polydomain textures should be taken into account in the present study. The optically and electrically anisotropic domains in the polydomain textures may be fully rotated or oscillated by the electric field with a frequency much lower than ν_1 , which was observed rheologically for a concentrated solution of PBLG [20]. However, the relaxations of other factors were superposed and no decisive results were found in figures 5 and 6. In any case, the broad relaxation at lower frequencies shown in figure 6 can be partially related to the limited angular diffusion of a rod within a virtual cone [13–16]. The relaxation around 10^6 Hz can be related to the transversal rotational-diffusion of a partially flexible rod with side chains as well as a local motion of chain segments in the relatively flexible rod confined in the concentrated solution.

3.3. Concentration dependence of the dielectric constant

The concentration dependences of ϵ_r' measured at 10^5 Hz and 10^6 Hz are shown in figure 7. In figure 7, the reported concentration for the onset of mesophase formation and biphasic region is indicated by arrow a. The upper concentration limit of the biphasic region is also indicated by arrow b [4–6]. No significant discontinuous changes in ϵ_r' measured at 10^5 Hz and 10^6 Hz can be observed in figure 7 at the concentrations around the onset of the isotropic–cholesteric phase transition and in the biphasic region. The dielectric constant measured at 10^5 Hz increases to show the maximum around 10 wt%, and it decreases linearly after the maximum. The linear dependence of ϵ_r' measured at 10^5 Hz after the maximum is expected to provide an in-situ monitoring method for the preparation process of solid films cast from aqueous solutions. The dielectric constant at 10^6 Hz decreases linearly as the concentration increases up to around 47 wt%, and it further decreases linearly but a little more steeply above 47 wt%. The critical concentration of 47 wt% can be

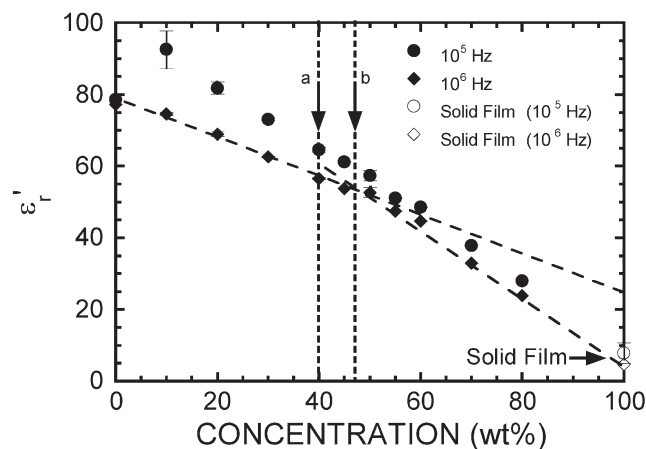


Figure 7. Concentration dependences of the dielectric constant, ϵ_r' , measured at 10^5 Hz and 10^6 Hz. The reported onset concentration of mesophase formation and the biphasic region is indicated by arrow a. The upper concentration limit of the biphasic region is indicated by arrow b [4–6].

consistently chosen at the intersection between the linear line extrapolated from 0 wt% and the linear line from 100 wt%.

The increase in ϵ_r' measured at 10^5 Hz around 10 wt% shows that the ionic species from HPC were dissolved in water, which qualitatively agrees well with the pH of 5.47 for the aqueous solution of 2 wt% reported by the supplier. The observed linear decrease after the maximum would be closely related to the decrease in the weight fraction of water, which has a larger value of ϵ_r' than HPC, and the decrease in the dissociation of the ionic species, which contributes apparently to the polarization. Therefore, the concentration dependence would be mainly controlled by a competition between the weight fraction of water and the dissociation of the ionic species. In addition, the increase in the solution viscosity with an increase in the concentration of HPC would be a (macroscopic) factor for the competition.

No significant effect of the dissociated ionic species on ϵ_r' measured at 10^6 Hz is observed in figure 7 because ϵ_r' decreases linearly as the concentration increases from 0 wt% to around 47 wt%. It is worth noting that ϵ_r' above 47 wt% HPC further decreases linearly but a little more steeply. The concentration of 47 wt% was not related to the onset of the isotropic–cholesteric phase transition and in the biphasic region. Rather, it was related to the fully developed cholesteric phase transition with the polydomain textures.

Below 47 wt%, ϵ_r' measured at 10^6 Hz would be mainly related to the transversal rotational-diffusion of a partially flexible rod with side chains, as shown in figure 1, assuming that the relaxation frequency of the longitudinal rotational-diffusion for HPC in water is

sufficiently lower, similar to that reported for HPC in dioxane [13]. In the biphasic region, the molecules in the isotropic portion can be fully rotated. On the other hand, the molecules are a little more confined in the anisotropic portion. However, the effect in the anisotropic portion would be negligibly small. Therefore, the concentration dependence below 47 wt% would be mainly controlled by the weight fraction of water.

Above 47 wt%, the cholesteric phase was fully developed over the solution. Further, polydomain textures were observed in figures 3 and 4. In the polydomain textures, anisotropic domains are randomly distributed. Then, the transversal rotational-diffusion of a partially flexible rod with side chains can be detected. A local motion of chain segments in the relatively flexible rod can also be detected as longitudinal component and/or transversal component even confined in the concentrated and anisotropic solutions. In addition, the relaxation of the rotation or oscillation of the anisotropic domains may be detected electrically at a frequency much lower than ν_1 relating to the size of the anisotropic domain [20]. At relatively higher frequencies, the transversal rotational-diffusion with side chains would be fully active in the diluted solutions below 47 wt%, whereas it would be restricted to some extent in the concentrated solutions prescribed by the neighbouring molecules in the anisotropic phase. Similarly, a local motion of chain segments in the diluted solutions would be fully active, whereas the local motion would be restricted in the concentrated and anisotropic solutions. It can be thought that the effect of the polydomain texture is also significant for the ϵ_r'' results, which are discussed in the next section.

3.4. Concentration dependence of the dielectric loss factor

Figures 8 a and 8 b show the concentration dependences of the dielectric loss factor, ϵ_r'' , measured at 10^5 Hz and 10^6 Hz, respectively. The arrows have the same meaning as those in figure 7. Both the dielectric loss factors measured at 10^5 Hz and 10^6 Hz show a broad peak around 20 wt%. Similar to the concentration dependences of ϵ_r' , no significant discontinuous changes in ϵ_r'' measured at 10^5 Hz and 10^6 Hz are found at the concentrations around the onset of the isotropic–cholesteric phase transition. In contrast, steeper decreases in ϵ_r'' can be observed around the critical concentration for the fully developed cholesteric phase.

As shown by equation (2), ϵ_r'' is mainly related to the conductance of the sample, G_s , at a given frequency. As

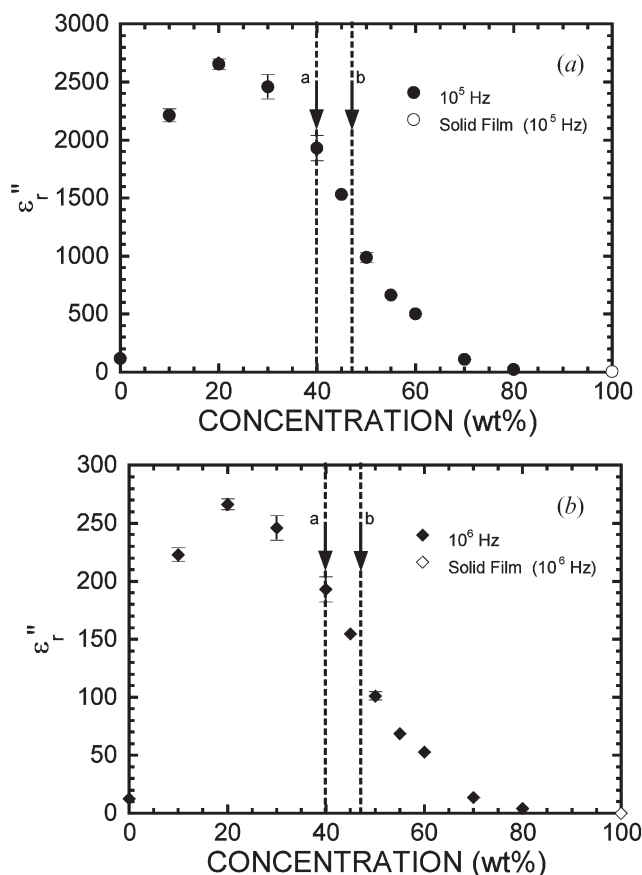


Figure 8. Concentration dependences of the dielectric loss factor, ϵ_r'' , measured at 10^5 Hz (a) and 10^6 Hz (b). The arrows have the same meaning as those in figure 7.

discussed in section 3.2, the effect of the dc conduction was not subtracted from the measured conductance although the dc conduction was relatively small at 10^5 Hz and 10^6 Hz.

Similar to the discussion in figure 7, the initial increases in ϵ_r'' shown in figure 8 are related to the increase in the ionic species dissolved from HPC, which contribute to the ionic conduction. The gradual decrease after the maximum up to 45 wt% would be related to the decreases in the weight fraction of water and the dissociation of the ionic species. The increase in the solution viscosity with an increase in the concentration of HPC would also be a factor for the decrease. However, no significant discontinuous changes in ϵ_r'' are found in figure 8 from 40 wt% to 45 wt%, concentrations at which the onset of the isotropic–cholesteric phase transition and the biphasic state are observed. At 40 wt%, anisotropic domains were found, as shown in figure 3 a, but the anisotropic domains were not fully developed over the solution. At concentrations around 45 wt% in the biphasic region, small anisotropic

spherulites were dominant, as shown in figure 4a, but an isotropic portion surrounding the anisotropic spherulites would act as a conduction path. In the case of shear-induced polydomain textures, as observed in figure 3b, the isotropic portion would be apparently hindered by the developed anisotropic portion, and the isotropic portion would similarly act as a conduction path. Since no significant discontinuous changes were observed in figure 8 in the biphasic region, the ionic species preferably move through the isotropic portion in the biphasic region, probably because the boundary between the isotropic portion and the anisotropic portion of the polydomain textures would act as potential barriers (or an excess resistance) for the conduction.

Above 47 wt%, the concentration at which the cholesteric phase is fully developed, the ionic species are forced to move across the boundary between the polydomain textures, which act as potential barriers for conduction. Analogous to the discussion for ionic conduction in solid films [17, 25–27], the potential barriers (or electrical inhomogeneities) would contribute to produce specially separated charges temporarily, and also contribute to the dielectric polarization or conduction losses. Further, the ionic conduction was relatively reduced for the concentrated solutions, and other broad relaxations were much more pronounced especially around 10^6 Hz, as shown in figure 5b (or figure 6). In the fully cholesteric phase, the molecular motions are also restricted, as discussed in section 3.2. The potential barriers for the ionic conduction as well as the restriction for the molecular motions would be significantly increased above 47 wt% in the fully developed cholesteric phase with polydomain textures.

Finally, the relationship between ϵ_r' and ϵ_r'' was also investigated. In figure 9, ϵ_r'' is plotted logarithmically against ϵ_r' . The discontinuous decreases in ϵ_r'' are much more pronounced at a critical dielectric constant indicated by the arrows, which is almost independent of the frequencies of 10^5 Hz and 10^6 Hz. The corresponding concentration for the critical dielectric constant was 50 wt% for the solution around the critical concentration. Therefore, the discontinuous decreases are not related to the onset of the isotropic–cholesteric phase transition but closely related to the fully developed cholesteric phase transition with polydomain textures.

4. Conclusions

In the present paper, the concentration dependences of dielectric properties measured at 10^5 Hz and 10^6 Hz are reported for aqueous solutions of hydroxypropyl

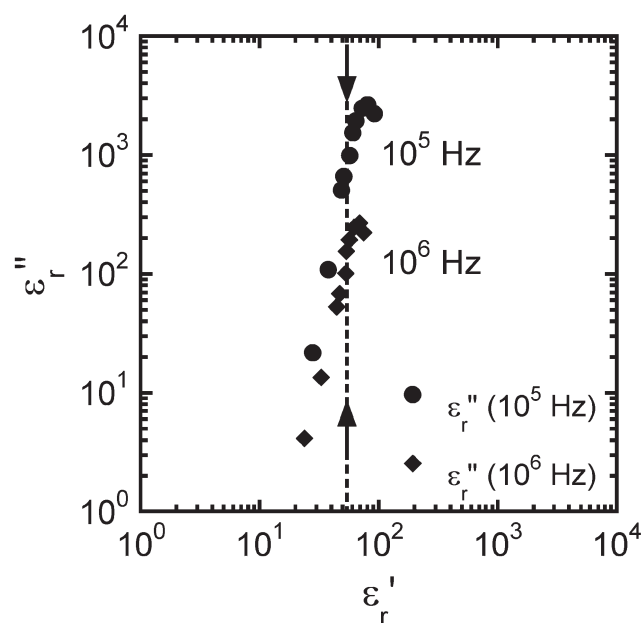


Figure 9. The dielectric loss factor, ϵ_r'' , plotted logarithmically against ϵ_r' measured at 10^5 Hz and 10^6 Hz. Discontinuous decreases in ϵ_r'' are indicated by the arrows.

cellulose (HPC). The phase behaviour of the solutions was also observed with a polarizing optical microscope. At a concentration of 45 wt% HPC, small anisotropic spherulites were observed, suggesting a biphasic state. Shear-induced textures including the banded texture were also observed for the concentrated solution of 80 wt% HPC. The dielectric relaxation properties in the cholesteric phase have been discussed in relation to the restricted molecular motion and the ionic conduction passing through the boundary of the polydomain textures. No significant discontinuous changes in ϵ_r' and ϵ_r'' were found at the concentrations around the onset of the isotropic–cholesteric phase transition and in the biphasic region. In contrast, the steeper changes in ϵ_r' and ϵ_r'' were found at the critical concentration for the fully developed cholesteric phase transition with polydomain textures. It should be noted that ϵ_r' measured at 10^5 Hz increased to show a maximum around 10 wt%, and it decreased linearly after the maximum. The linear dependence of ϵ_r' measured at 10^5 Hz after the maximum is expected to provide an in-situ monitoring method for the preparation process of solid films cast from aqueous solutions.

Acknowledgments

This work was partially supported by a Grant-in-Aid for Scientific Research from the Japan Society for the Promotion of Science. We are also grateful to

Dr. Shimura (TOSOH Analysis and Research Centre Co.) for the dielectric measurements of the solid films.

References

- [1] R.S. Werbowyj, D.G. Gray. *Mol. Cryst. liq. Cryst.*, **34**, 97 (1976).
- [2] R.S. Werbowyj, D.G. Gray. *Macromolecules*, **13**, 69 (1980).
- [3] R.S. Werbowyj, D.G. Gray. *Macromolecules*, **17**, 1512 (1984).
- [4] G. Conio, E. Bianchi, A. Ciferri, A. Tealdi, M.A. Aden. *Macromolecules*, **16**, 1264 (1983).
- [5] F. Fried, P. Sixou. *J. Polym. Sci. Polym. Chem. Ed.*, **22**, 239 (1984).
- [6] S. Guido. *Macromolecules*, **28**, 4530 (1995).
- [7] R.J. Samuels. *J. Polym. Sci. A-2*, **7**, 1197 (1969).
- [8] L.-O. Sundelöf, B. Nyström. *J. Polym. Sci. Polym. Lett. Ed.*, **15**, 377 (1977).
- [9] H.G. Shinouda, M.M.A. Moteleb. *J. appl. Polym. Sci.*, **98**, 571 (2005).
- [10] D. Meißner, J. Einfeldt, A. Kwasniewski. *J. non-crystalline Solids*, **275**, 199 (2000).
- [11] A. Rachocki, E. Markiewicz, J. Tritt-Goc. *Acta phys. Polonica A*, **108**, 137 (2005).
- [12] M. Pizzoli, M. Scandola, G. Ceccorulli. *Plast. Rubb. Composites Processing Applic.*, **16**, 239 (1991).
- [13] M.M.A. Moteleb, M.M. Naoum, M.M. Shalaby, G.R. Saad. *Polym. Int.*, **34**, 363 (1994).
- [14] J.K. Moscicki, G. Williams, S.M. Aharoni. *Macromolecules*, **15**, 642 (1982).
- [15] M.P. Warchol, W.E. Vaughan. *Adv. mol. Relaxation Interaction Processes*, **13**, 317 (1978).
- [16] C.C. Wang, R. Pecora. *J. chem. Phys.*, **72**, 5333 (1980).
- [17] J. Einfeldt, D. Meißner, A. Kwasniewski. *J. non-crystalline Solids*, **320**, 40 (2003).
- [18] J.-B. Riti, P. Navard. *J. Rheol.*, **42**, 225 (1998).
- [19] K. Tanaka, K. Yonetake, T. Masuko, R. Akiyama. *J. Macromol. Sci. B*, **42**, 901 (2003).
- [20] K. Tanaka, A. Takahashi, R. Akiyama. *Phys. Rev. E*, **58**, R1234 (1998).
- [21] K. Tanaka, Y. Tanabe, T. Morina, R. Akiyama, submitted.
- [22] For instance, R.C. Weast (Ed.), *CRC Handbook of Chemistry and Physics* 57th edn, CRC Press, Cleveland (1977).
- [23] F. Perrin. *J. Phys. Radium*, **5**, 497 (1934).
- [24] A. Wada. *J. chem. Phys.*, **30**, 329 (1959).
- [25] H.E. Taylor. *Trans. Faraday Soc.*, **52**, 873 (1956).
- [26] J.M. Stevels. *J. non-crystalline Solids*, **40**, 69 (1980).
- [27] K. Yamamoto, H. Namikawa. *Jap. J. appl. Phys.*, **27**, 1845 (1988).